JHEP

Published for SISSA by Springer

Received: July 19, 2013
Revised: December 13, 2013
Accepted: December 13, 2013
Published: January 9, 2014

LHC data and aspects of new physics

Tommi Alanne,[a,b] **Stefano Di Chiara**[a] **and Kimmo Tuominen**[a,b]

[a] *Helsinki Institute of Physics, Univ. of Helsinki,*
P.O. Box 64, FI-000140 Helsinki, Finland
[b] *Department of Physics, Univ. of Jyväskylä,*
P.O. Box 35, FI-40014 Jyväskylä, Finland

E-mail: tommi.alanne@jyu.fi, stefano.dichiara@helsinki.fi, kimmo.i.tuominen@jyu.fi

Abstract: We consider the implications of current LHC data on new physics with strongly interacting sector(s). We parametrize the relevant interaction Lagrangian and study the best fit values in light of current data. These are then considered within a simple framework of bosonic technicolor. We consider first the effective Lagrangian containing only spin-0 composites of the underlying theory, which corresponds to a two Higgs doublet model. With respect to this baseline, the effects of the vector bosons, a staple in strong interacting theories, are illustrated by considering two cases: first, the case where the effects of the vector bosons arise only through their mixing with the electroweak $SU(2)_L$ gauge fields and, second, the case where also a direct interaction term with neutral scalars exists. We find that the case with a direct coupling of the composite vector fields to the Higgs allows the tested model to fit the experimental results with goodness comparable to that of the SM.

Keywords: Phenomenological Models

ArXiv ePrint: 1303.3615

doi:10.1007/JHEP01(2014)041

JHEP01(2014)041

Contents

1 Introduction

The recent discovery of a light scalar with properties compatible with those of the Standard Model (SM) Higgs boson, h^0, imposes new experimental tests on previously viable beyond the Standard Model (BSM) theory frameworks. Fervent activity in this direction has focused mostly on the possibility that a new charged particle could enhance the Higgs decay rate to two photons [1–13]. This is measured at LHC and Tevatron, with the full dataset, to be slightly enhanced compared to the SM prediction [14–17], with the diphoton signal strength equal to 1.55 ± 0.31 at ATLAS and 0.78 ± 0.28 at CMS. While most of the efforts were focused on the Higgs physics associated with a new charged scalar or a vector fermion, both of which naturally arise in supersymmetry [18–24] or composite Higgs frameworks [25–28], less extensive research has been conducted recently on the possibility that a heavy charged vector boson be responsible for the observed deviations of the Higgs couplings from the corresponding SM predictions [9, 29–31].

A heavy charged vector boson is naturally predicted by phenomenological theories featuring additional gauge groups, like Technicolor, Little Higgs, and Kaluza-Klein models [32–37]. In this paper we want to explore the effect of couplings of a heavy W' boson to the Higgs on LHC and Tevatron observables. To approach this task we first, in section 2, perform a fit with the parameters of a simple effective Lagrangian featuring rescaled Higgs couplings to SM particles as well as to a heavy charged scalar and a heavy charged vector boson. To have a concrete model to test against the results of the general fit, in section 3 we introduce a low energy effective Lagrangian for a simple bosonic technicolor model, the bosonic Next to Minimal Walking Technicolor (bNMWT) [38–41]. The low energy effective Lagrangian for the scalar sector of bNMWT corresponds to a Type-I Two Higgs Doublet

JHEP01(2014)041

ij	ATLAS	CMS	Tevatron
ZZ	1.43 ± 0.38	0.91 ± 0.28	
$\gamma\gamma$	1.55 ± 0.31	0.78 ± 0.28	6.0 ± 3.30
WW	0.99 ± 0.30	0.76 ± 0.21	0.94 ± 0.84
$\tau\tau$	0.70 ± 0.70	1.10 ± 0.41	
bb	0.2 ± 0.7	1.00 ± 0.49	1.59 ± 0.71

Table 1. Data on inclusive channels from LHC and Tevatron experiments.

Model (2HDM) [42]. We scan the allowed parameter space of this model for data points viable under direct search constraints and electroweak (EW) precision tests, compare the data points to the measured Higgs physics observables, and find the optimal fit of the model. In section 4 we introduce two composite vector boson triplets in the low energy Lagrangian, while conserving gauge invariance at the microscopic level, which both mix with the SM $W^{\pm}$ and directly couple to h^0, and repeat the goodness of fit analysis above to determine the optimal values of the W' and W'' couplings to h^0. We illustrate separately the features which originate from the mixing and from the direct coupling. Our essential conclusion is that mixing alone produces a negligible change of the fit to the current data, while a direct interaction gives a more relevant improvement of the fit, at a level of goodness comparable to that of the SM.

2 LHC and Tevatron data fit

In this section we perform a fit to LHC and Tevatron data to determine the values of the Higgs couplings favored by the experiment. We follow the methods of previous similar analyses [1–13] while updating their results with the latest experimental data, featuring up to $8\,\text{fb}^{-1}$ of additional integrated luminosity relatively to the previous datasets. The following model-independent analysis serves as a comparison with the model-specific goodness of fit study we perform in sections 3, 4.

The experimental results are expressed in terms of the signal strengths, defined as

$$\hat{\mu}_{ij} = \frac{\sigma_{\text{tot}}\text{Br}_{ij}}{\sigma_{\text{tot}}^{\text{SM}}\text{Br}_{ij}^{\text{SM}}}\,, \quad \sigma_{\text{tot}} = \sum_{\Omega=h,qqh,\ldots} \epsilon_{\Omega}\sigma_{\omega\to\Omega}\,, \quad \omega = pp, p\bar{p}\,, \tag{2.1}$$

where ϵ_Ω is the efficiency associated with the given final state Ω in an exclusive search, while for inclusive searches one simply has $\sigma_{\text{tot}} = \sigma_{pp\to h(X)}$, the h production total cross section. The signal strengths from ATLAS, CMS, and Tevatron are given in table 1. All results above for Higgs decays at ATLAS [43, 44] and CMS [15, 45], as well as those at the Tevatron [16, 17], use the full respective dataset, with the only exception being the coupling strength for the decay to $\tau\bar{\tau}$ at ATLAS [46] which uses 13 fb^{-1} of integrated luminosity at 8 TeV and 5 fb^{-1} at 7 TeV. The $b\bar{b}$ quark pair is produced in association with a vector boson, with an efficiency assumed equal to one, while the other searches are

JHEP01(2014)041

	ATLAS 7TeV	ATLAS 8TeV	CMS 7TeV	CMS 8TeV
$\gamma\gamma JJ$	2.7 ± 1.9	2.8 ± 1.6	4.2 ± 2.0	0.8 ± 1.0
$pp \to h$	22.5%	45.0%	26.8%	46.8%
$pp \to qqh$	76.7%	54.1%	72.5%	51.1%
$pp \to t\bar{t}h$	0.6%	0.8%	0.6%	1.7%
$pp \to Vh$	0.1%	0.1%	0%	0.5%

Table 2. Data on exclusive channels from LHC experiments.

inclusive. We also include in our analysis the dijet associated $\gamma\gamma$ production based on the full dataset [14, 15], with signal strengths and efficiencies[1] listed in table 2.

Within the class of models we will study, the part of the Lagrangian relevant for the recent LHC data is of the form

$$\mathcal{L}_{\text{eff}} = a_V \frac{2m_W^2}{v_w} h W_\mu^+ W^{-\mu} + a_V \frac{m_Z^2}{v_w} h Z_\mu Z^\mu - a_f \sum_{\psi=t,b,\tau} \frac{m_\psi}{v_w} h \bar{\psi}\psi$$
$$+ a_{V'} \frac{2m_{W'}^2}{v_w} h W_\mu'^+ W'^{-\mu} - a_S \frac{2m_S^2}{v_w} h S^+ S^-, \tag{2.2}$$

where the fourth and fifth terms involve, respectively, charged (but color singlet) vector and scalar bosons. We fix the mass parameters to the physical mass of the corresponding particle and v_w to the EW vacuum expectation value (vev), $v_w = 246\,\text{GeV}$.

Application of the Lagrangian in eq. (2.2) in our study requires on one hand that the dimensionless couplings, i.e. the Yukawas, are sufficiently small. Practically one needs only worry about the coupling of the top quark, and in our numerical analysis we demonstrate explicitly that on the average over the viable part of the parameter space we have $y_t = \sqrt{2} a_f m_t / v_w \sim 1$. On the other hand, we must require that the masses of the composite vectors and charged scalars are smaller than the cutoff scale below which the effective description is expected to be valid. In our analysis we choose the cutoff scale to be $\Lambda_{TC} \sim 4\pi v_w \sim 3\,\text{TeV}$. The effects of composite vectors and charged scalars in our results are parametrized only in terms of the dimensionless coefficients $a_{V'}$ and a_S provided that the states W' and $S^\pm$ are sufficiently heavy; see the discussion around eqs. (2.5)–(2.8). In the model considered in section III and IV this requirement is satisfied since the composite states originating from a new strongly interacting sector naturally have their masses in the TeV range.

Consequently to eq. (2.2), the cross sections and branching rates relevant for Higgs physics are related to the corresponding quantities of the SM in a simple way. We define

$$\hat{\Gamma}_{ij} \equiv \frac{\Gamma_{h\to ij}}{\Gamma^{\text{SM}}_{h_{\text{SM}}\to ij}}, \quad \hat{\sigma}_\Omega \equiv \frac{\sigma_{\omega\to\Omega}}{\sigma^{\text{SM}}_{\omega\to\Omega}}, \tag{2.3}$$

and then, in terms of the coupling coefficients in eq. (2.2), we have

$$\hat{\sigma}_{hqq} = \hat{\sigma}_{hA} = \hat{\Gamma}_{AA} = |a_V|^2, \qquad \hat{\sigma}_{h\bar{t}t} = \hat{\sigma}_h = \hat{\Gamma}_{gg} = \hat{\Gamma}_{\psi\psi} = |a_f|^2,$$
$$A = W, Z; \qquad \psi = b, \tau, c, \ldots \tag{2.4}$$

[1] We include only the loose categories from the ATLAS and CMS dataset at 8 TeV.

JHEP01(2014)041

where the gg and h final states are produced through a loop triangle diagram with only quarks as virtual particles.

The calculation of the Higgs decay rate to two photons is more involved. By using the formulas given in [47], we can write

$$\Gamma_{h\to\gamma\gamma} = \frac{\alpha_e^2 m_h^3}{256\pi^3 v_w^2}\left|\sum_i N_i e_i^2 F_i\right|^2 , \tag{2.5}$$

where the index i is summed over the SM charged particles as well as $S^\pm$ and $W'^\pm$, N_i is the number of colors, e_i the electric charge in units of the electron charge, and the factors F_i are defined by

$$\begin{aligned} F_A &= [2 + 3\tau_A + 3\tau_A\,(2-\tau_A)\,f(\tau_A)]\,a_V\,, & A &= W, W'\,; \\ F_\psi &= -2\tau_\psi\,[1 + (1-\tau_\psi)\,f(\tau_\psi)]\,a_f\,, & \psi &= t, b, \tau, \ldots\,; \\ F_S &= \tau_S\,[1 - \tau_S f(\tau_S)]\,a_S\,, & \tau_i &= \frac{4m_i^2}{m_h^2}\,, \end{aligned} \tag{2.6}$$

with

$$f(\tau_i) = \begin{cases} \arcsin^2\sqrt{1/\tau_i} & \tau_i \geq 1 \\ -\dfrac{1}{4}\left[\log\dfrac{1+\sqrt{1-\tau_i}}{1-\sqrt{1-\tau_i}} - i\pi\right]^2 & \tau_i < 1 \end{cases} . \tag{2.7}$$

In the limit of heavy $W'^\pm$ and $S^\pm$, one finds

$$F_{W'} = 7a_{V'}\,, \quad F_S = -\frac{1}{3}a_S. \tag{2.8}$$

Given the experimental lower bounds on $m_{W'}$ and m_S [48, 49], the error on $F_{W'}$ is irrelevant while $|F_S|$ gets enhanced by about 10% for $m_S = 150\,\text{GeV}$: since the experimental error on $\hat{\mu}_{\gamma\gamma}$ is large and constructive interference of the $S^\pm$ and $W^\pm$ is favored by the experiment, we also assume the error involved by the above approximation for F_S to be negligible.

We notice also that in the limit of heavy masses for the charged scalar and vector bosons the light Higgs decay to such (virtual) states is highly suppressed by kinematics, and therefore no additional decay channels have to be taken into account besides those of the SM.

To evaluate the theoretical predictions for the measured observables, we need the SM production cross sections for the Higgs boson and the SM branching ratios for its decay. The production cross sections of a Higgs boson with a 125 GeV mass at the LHC and Tevatron for the final state Ω are given [50] in table 3.

The SM branching fractions are defined in terms of the decay rates, $\Gamma^{\rm SM}_{h\to ij}$, as

$$\text{Br}^{\rm SM}_{ij} = \frac{\Gamma^{\rm SM}_{h\to ij}}{\Gamma^{\rm SM}_{\rm tot}}\,, \quad \Gamma^{\rm SM}_{\rm tot} = \sum_{ij=\bar{b}b,gg,WW,\ldots} \Gamma^{\rm SM}_{h\to ij} = 4.03\text{MeV}. \tag{2.9}$$

These are given [51] by

$$\text{Br}^{\rm SM}_{b\bar{b}} = 0.578, \quad \text{Br}^{\rm SM}_{\tau\bar{\tau}} = 0.0637, \quad \text{Br}^{\rm SM}_{c\bar{c}} = 0.0268, \quad \text{Br}^{\rm SM}_{gg} = 0.0856, \tag{2.10}$$

$$\text{Br}^{\rm SM}_{\gamma\gamma} = 0.0023, \quad \text{Br}^{\rm SM}_{\gamma Z} = 0.00155, \quad \text{Br}^{\rm SM}_{WW} = 0.216, \quad \text{Br}^{\rm SM}_{ZZ} = 0.0267. \tag{2.11}$$

JHEP01(2014)041

Ω	h	qqh	$t\bar{t}h$	Wh	Zh	$h(X)$
7 TeV	15.31	1.211	0.08634	0.5729	0.3158	17.50
8 TeV	19.52	1.578	0.1302	0.6966	0.3943	22.32
1 TeV	0.9493	0.0653	0.0043	0.1295	0.0785	1.227

Table 3. Standard Model Higgs production cross sections in units of pb.

To determine the experimentally favored values of the free parameters $a_f, a_V, a_{V'}, a_S$, we minimize the quantity

$$\chi^2 = \sum_i \left(\frac{\mathcal{O}_i^{\rm exp} - \mathcal{O}_i^{\rm th}}{\sigma_i^{\rm exp}} \right)^2 , \tag{2.12}$$

where the measured values and errors of the observables are given in tables 1, 2, while the numerical predictions of the theory are easily determined from eqs. (2.3)–(2.8), with the SM input values given in table 3. In defining χ^2 above, we assumed the correlation matrix to be simply the identity matrix. We note that it is not possible to constrain both a_S and $a_{V'}$ since they both contribute only to the diphoton decay. The optimal values given below then refer to either of the two taken equal to zero:

$$a_V = 0.96^{+0.10}_{-0.11}\,, \qquad a_f = 1.01^{+0.25}_{-0.33}, \qquad \begin{cases} a_{V'} = 0.21^{+0.16}_{-0.18} \text{ and } a_S = 0 \\ a_{V'} = 0 \text{ and } a_S = -2.7^{+3.9}_{-3.3} \end{cases} , \tag{2.13}$$

with

$$\chi^2_{\rm min}/\text{d.o.f.} = 1.04\,, \quad P\left(\chi^2 > \chi^2_{\rm min}\right) = 41\%\,, \quad \text{d.o.f.} = 14. \tag{2.14}$$

The results above are derived in the limit of heavy $S^\pm$ and $W'^\pm$. For masses of the same order of m_h the optimal a_S and $a_{V'}$ can be straightforwardly derived by dividing the corresponding values in eqs. (2.13) by the ratio of the decay amplitudes $F_{W'}$ and F_S, eqs.(2.6), divided each by their respective heavy particle limits given in eqs. (2.8). We stress that because of the limited number of observables used in the analysis and the fact that possible systematic errors are unaccounted for, the P-value quoted above (and also the ones evaluated in the subsequent section) should be used exclusively to compare the models studied in this work with the SM.

The SM produces

$$\chi^2_{\rm min}/\text{d.o.f.} = 0.92\,, \quad P\left(\chi^2 > \chi^2_{\rm min}\right) = 55\%\,, \quad \text{d.o.f.} = 17\,, \tag{2.15}$$

for only the Higgs physics data, which indeed is a rather ideal result. The inclusion of the EW parameters S and T ($S = T = 0$ for SM) [52–54] in the fit improves further the quality of the fit:

$$\chi^2_{\rm min}/\text{d.o.f.} = 0.89\,, \quad P\left(\chi^2 > \chi^2_{\rm min}\right) = 60\%\,, \quad \text{d.o.f.} = 19, \tag{2.16}$$

which shows that the SM is still perfectly viable in light of current collider data.

In the next section we use the Higgs physics constraints derived here to test the viability of a simple bosonic walking technicolor model [41] whose low energy effective Lagrangian belongs to the class specified by the generic Lagrangian of eq. (2.2).

JHEP01(2014)041

3 Model and constraints

In Technicolor (TC) an additional, confining gauge interaction causes techniquarks, charged under TC and the EW interaction, to condense and break spontaneously the EW symmetry [32, 33]. This mechanism allows the W and Z bosons, and the composite states of the strongly coupled TC sector to acquire mass, while the SM fermions remain massless.

The TC sector we consider has $\mathrm{SU}(2)_L \times \mathrm{SU}(2)_R$ chiral symmetry and is described in terms of the complex composite meson field $M^T = (\phi^+, \phi^0)$ by an effective Lagrangian

$$\mathcal{L}_{\mathrm{TC}} = D_\mu M^\dagger D^\mu M - m_M^2 M^\dagger M - \frac{\lambda_M}{3!}\left(M^\dagger M\right)^2 . \tag{3.1}$$

To provide mass for ordinary matter fermions, an additional interaction linking them to the TC condensate has to be provided. In bosonic TC models, this link is provided by one (or more) elementary scalar(s) [55–59]. While in this paper we consider nonsupersymmetric theories, bosonic technicolor effective Lagrangians also arise as low energy realizations of supersymmetric technicolor theories [60–62]. In the context of bosonic TC, it is therefore the techniquark condensate that breaks EW symmetry, while the scalar plays the role of "spectator". The Higgs Lagrangian is written in terms of the usual complex doublet H as

$$\mathcal{L}_{\mathrm{Higgs}} = D_\mu H^\dagger D^\mu H - m_H^2 H^\dagger H - \frac{\lambda_H}{3!}\left(H^\dagger H\right)^2 . \tag{3.2}$$

The link between the technicolor and the SM matter fields obtained at the effective Lagrangian level is due to the Yukawa couplings of the Higgs field H. In addition to the usual couplings to the SM matter fields,

$$\mathcal{L}_{\mathrm{Yuk}} = (y_u)_{ij} H \bar{Q}_i U_j + (y_d)_{ij} H^\dagger \bar{Q}_i D_j + (y_\ell)_{ij} H^\dagger \bar{L}_i E_j + \mathrm{h.c.}\,, \tag{3.3}$$

these include also the couplings to techniquarks, $y_{TC}\bar{\Psi}_L H \Psi_R$. When constructing the effective Lagrangian for the composite sector of the theory, this coupling generates further terms in the effective TC Lagrangian so that the technicolor sector is described by [41][2]

$$\begin{aligned}\mathcal{L}_{\mathrm{bTC}} = {} & D_\mu M^\dagger D^\mu M - m_M^2 M^\dagger M - \frac{\lambda_M}{3!}\left(M^\dagger M\right)^2 \\ & + \Big[c_3 y_{TC} D_\mu M^\dagger D^\mu H + c_1 y_{TC} f^2 M^\dagger H + \frac{c_2 y_{TC}}{3!}(M^\dagger M)(M^\dagger H) \\ & + \frac{c_4 y_{TC}}{3!}\lambda_H (H^\dagger H)(M^\dagger H) + \mathrm{h.c.}\Big]\,,\end{aligned} \tag{3.4}$$

where c_i are unknown parameters and f is the vev of M. Since eq. (3.4) is an effective Lagrangian description, its parameters are supposed to encode higher order and nonperturbative corrections from the underlying theory. This justifies the application of the model at tree level in our study.

The model that we consider is therefore specified by the effective Lagrangian

$$\mathcal{L} = \mathcal{L}_{\mathrm{SM}} + \mathcal{L}_{\mathrm{bTC}}, \tag{3.5}$$

[2] Compared to the potential presented in [41], expressed in terms of matrix fields rather than EW doublets, we absorbed the ω factors in the c_i coefficients and pulled out a factor λ_H in front of c_4, as suggested by naive dimensional analysis.

JHEP01(2014)041

where $\mathcal{L}_{\rm SM}$ is the usual SM Lagrangian containing the sectors $\mathcal{L}_{\rm Higgs}$ and $\mathcal{L}_{\rm Yuk}$. The coefficients c_i in eq. (3.4) are estimated by naive dimensional analysis [63, 64] to be

$$c_1 \sim \omega\,, \quad c_2 \sim \omega\,, \quad c_3 \sim \omega^{-1}\,, \quad c_4 \sim \omega^{-1}\,; \quad \omega \lesssim 4\pi\,. \tag{3.6}$$

Two of the parameters on the r.h.s. of eqs. (3.2), (3.4) are determined by the extremum conditions of the potential. Furthermore, the electroweak scale constrains the vevs of M and H by

$$v_w^2 = v^2 + f^2 + 2c_3 y_{TC} f v = (246\ \text{GeV})^2\,, \quad \langle M\rangle = \frac{f}{\sqrt{2}}\,, \quad \langle H\rangle = \frac{v}{\sqrt{2}}\,. \tag{3.7}$$

Finally, the requirement for the potential to be bounded from below imposes

$$\lambda_H, \lambda_M > 0\,; \quad \lambda_H + \lambda_M > 2\,(c_2 + c_4\lambda_H)\,y_{TC}. \tag{3.8}$$

The mass eigenstates are obtained by diagonalizing first the kinetic terms and then applying a rotation to diagonalize the mass terms in the scalar and pseudoscalar sectors. First, the Higgs fields M and H are expressed as

$$\begin{pmatrix} M \\ H \end{pmatrix} = \frac{1}{\sqrt{2}} \begin{pmatrix} A & B \\ -A & B \end{pmatrix} \begin{pmatrix} M_2 \\ M_1 \end{pmatrix}, \quad A = (1 - c_3 y_{TC})^{-1/2},\ B = (1 + c_3 y_{TC})^{-1/2}. \tag{3.9}$$

After this transformation, the fields $M_{1,2}$ are written in terms of the charge eigenstates as

$$M_{1,2} = \begin{pmatrix} \Sigma^{\pm}_{1,2} \\ \frac{1}{\sqrt{2}}(f_{1,2} + \sigma_{1,2} + i\xi_{1,2}) \end{pmatrix}. \tag{3.10}$$

The rotation angles α and β determine the physical states in the scalar and pseudoscalar sectors so that the Goldstone bosons, $G^{\pm}$ and G^0, provide the respective longitudinal components of the $W^{\pm}$ and Z bosons, while h^0, H^0, A^0, and $H^{\pm}$ are the neutral scalars, pseudoscalar, and charged scalar mass eigenstates, respectively:

$$\begin{pmatrix} h^0 \\ H^0 \end{pmatrix} = \begin{pmatrix} c_\alpha & -s_\alpha \\ s_\alpha & c_\alpha \end{pmatrix} \begin{pmatrix} \sigma_2 \\ \sigma_1 \end{pmatrix}, \ \begin{pmatrix} G^0 \\ A^0 \end{pmatrix} = \begin{pmatrix} s_\beta & c_\beta \\ c_\beta & -s_\beta \end{pmatrix} \begin{pmatrix} \xi_2 \\ \xi_1 \end{pmatrix}, \ \begin{pmatrix} G^{\pm} \\ H^{\pm} \end{pmatrix} = \begin{pmatrix} s_\beta & c_\beta \\ c_\beta & -s_\beta \end{pmatrix} \begin{pmatrix} \Sigma^{\pm}_2 \\ \Sigma^{\pm}_1 \end{pmatrix}. \tag{3.11}$$

The mixing angle β is defined so that $\tan\beta = f_2/f_1$. The masses of the lightest composite states, including neutral scalars, are naturally expected to be of $O(\Lambda_{TC}) \sim 1\,\text{TeV}$. For bosonic TC the strong dynamics effect on the Higgs mass can be somewhat tamed by the mixing of the composite and elementary neutral scalar states, since the latter state can have a squared mass term much smaller than the former. This mechanism is analogous to the TeV-scale seesaw recently put forward in [65]. Moreover, it has been shown [66] that the top-quark loop contribution can greatly reduce the tree level TC prediction on the Higgs mass. A further suppression of the light Higgs mass is expected in NMWT because of walking dynamics [39]. From here on we assume that one or a combination of

JHEP01(2014)041

the mechanisms above is at work and use $m_{h^0} = 125 \pm 1\,\text{GeV}$ as an input to fix the value of one of the free parameters of the low energy effective theory.

To compare the model predictions with the LHC and Tevatron measurements, we need the coefficients of the SM Higgs linear couplings introduced in eq. (2.2) to be expressed in terms of the bNMWT parameters:

$$\begin{aligned} a_S \,=\, & \Big[(c_{2\beta}-c_{2\rho})\Big((c_2-c_4\lambda_H)\,c_\rho^{-1}s_\rho^{-1}\,(c_{\alpha+3\beta}+c_{\alpha-\beta}c_{2\beta}c_{2\rho}) \\ & \qquad +4\,(c_2+c_4\lambda_H)\,c_\beta s_\beta\,\big(c_\alpha c_\beta t_\rho^{-2}+s_\alpha s_\beta t_\rho^2\big)\Big) \\ & -\Big(c_{\alpha-\rho}s^2_{2(\beta-\rho)}s_{\beta+\rho}\lambda_H + c_{\alpha+\rho}s_{\beta-\rho}s^2_{2(\beta+\rho)}\lambda_M\Big)\,c_\rho^{-2}s_\rho^{-2}/y_{TC}\Big] \\ & /\left[4\left(c_4\lambda_H s^2_{\beta-\rho}+(12c_1+c_2)\,s^2_{\beta+\rho}\right)\right]\,, \\ a_V \,=\, & s_{\beta-\alpha}\,, \quad a_f = \frac{c_{\alpha-\rho}}{s_{\beta-\rho}}\,, \end{aligned} \tag{3.12}$$

where $s_\alpha, c_\alpha, t_\alpha$ are shorthands for $\sin\alpha, \cos\alpha, \tan\alpha$, respectively, with α, β defined by the rotation matrices in eq. (3.11) and ρ by

$$s_\rho = \sqrt{\frac{1-c_3 y_{TC}}{2}}\,, \quad c_\rho = \sqrt{\frac{1+c_3 y_{TC}}{2}}\,. \tag{3.13}$$

We are now ready to test the particle spectrum and its couplings against the latest experimental data. First, we scan the parameter space looking for data points that produce the right SM mass spectrum and satisfy the direct searches for charged particles at LEP [49] and a heavy neutral scalar at LHC [67] as well as the EW precision constraints from the S and T parameters [52–54]. More specifically, we impose the constraints

$$\begin{aligned} & m_{h^0} = 125 \pm 1\ \text{GeV}\,,\ m_{H^\pm} = m_{A^0} > 100\ \text{GeV}\,,\ m_{H^0} > 600\ \text{GeV}\,,\ \Big|\frac{s_{\alpha-\rho}}{s_{\beta-\rho}}\Big| < 1\,, \\ & S = 0.04 \pm 0.09\,,\ T = 0.07 \pm 0.08\,,\ r(S,T) = 88\%\,,\ m_{A^0}, m_{H^0} < 5\Lambda_{TC}\,. \end{aligned} \tag{3.14}$$

The quantity $r(S,T)$ is the correlation coefficient for the S and T parameters [54]. The constraint on the trigonometric functions is to ensure that the heavy Higgs does not couple to SM fermions more strongly than a SM Higgs with the same mass does; this allows us to use straightforwardly the LHC constraint on m_{H^0}. The upper bounds on m_{A^0}, m_{H^0} are enforced by the cutoff of $O(\Lambda_{TC} \approx 4\pi v_w)$ of the effective Lagrangian. We also require the free parameters to produce the remaining SM mass spectrum and satisfy the bounds in eq. (3.8). Then, we scan for such viable points in the domain

$$\begin{aligned} & 0 < \lambda_H, \lambda_M < (4\pi)^2\,,\ 2\pi < |c_1|, |c_2|, |c_3^{-1}|, |c_4^{-1}| < 8\pi\,,\ |c_3 y_{TC}| < 1 \\ & |y_t| < 4\pi\,,\ f = \pm\sqrt{v_w^2 - v^2\left(1-c_3^2 y_{TC}^2\right)} - v c_3 y_{TC}\,, |v| < v_w(1-c_3^2 y_{TC}^2)^{-1/2}\,, \end{aligned} \tag{3.15}$$

with m_H^2, m_M^2 determined by the extremum conditions

$$\frac{\partial V}{\partial h^0} = 0\,, \quad \frac{\partial V}{\partial H^0} = 0, \tag{3.16}$$

where V is the scalar potential of the effective Lagrangian in eqs. (3.2), (3.4), (3.5). The results that we present in the following of this section can be applied directly to the Type-I

JHEP01(2014)041

2HDM by using the formulas in appendix A. The disclaimer is that we are testing only a portion of the parameter space available to such a model, and more precisely the range of values typical for underlying strong dynamics.

Note that the value of y_t is fixed by the Higgs sector, and in the scan we only monitor that its value remains below 4π. Actually, over the scanned 5000 viable points, we find that on the average $y_t = 0.92 \pm 0.17$ with the maximum (minimum) value being 1.48 (0.27). Hence, the leading order perturbative treatment of the top Yukawa coupling which we have applied in our analysis is justified.

We also check that the perturbative calculation of the diphoton decay rate holds for each of the 5000 scanned data points. In doing so we perform a rough estimate of the loop amplitudes by assuming the virtual particles to have momenta much smaller then their masses and then by integrating the phase space volume up to the typical energy of the process, which is equal to the light Higgs mass. While such an estimate misses the enhancement of the amplitude given by on-shell virtual particles and the contribution of high momenta, it still allows us to compare the relative order of magnitude of the two loop contributions to the one loop order amplitude. The leading order contribution to the Higgs decay amplitude to two photons is given by a virtual W at one loop, which we simply label $\mathcal{A}_W^{1L}$. At next to leading order virtual scalars at two loops give the largest contribution, since the cubic couplings can be of $O(v_w 4\pi)^2$, while the other relevant couplings are SM-like in size. Scalar cubic and quartic couplings, both large, might indeed give non-perturbative contributions at even higher order. For this reason, besides the ratio between the two loop leading contribution in figure 1 ($\mathcal{A}_s^{2L}$) and $\mathcal{A}_W^{1L}$, we also calculate the ratio between $\mathcal{A}_s^{2L}$ and the virtual $H^\pm$ contribution at one loop ($\mathcal{A}_{H^\pm}^{1L}$), both of which are given below:

$$\frac{\mathcal{A}_s^{2L}}{\mathcal{A}_W^{1L}} \sim \frac{\lambda_{h^0h^0h^0}\lambda_{h^0H^+H^-}^2}{8\pi^2 a_V}\frac{v_w^4 m_W^4}{m_{H^\pm}^8}\,, \quad \frac{\mathcal{A}_s^{2L}}{\mathcal{A}_{H^\pm}^{1L}} \sim \frac{\lambda_{h^0h^0h^0}\lambda_{h^0H^+H^-}}{8\pi^2}\frac{v_w^2}{m_{H^\pm}^2}\,, \tag{3.17}$$

with

$$\lambda_{ijk} = \frac{1}{2v_w}\partial_{ijk}V\ . \tag{3.18}$$

To ensure consistency of the perturbative calculation of the light Higgs decay rate to diphoton, we require

$$\frac{\mathcal{A}_s^{2L}}{\mathcal{A}_W^{1L}} < 0.1\,, \quad \frac{\mathcal{A}_s^{2L}}{\mathcal{A}_{H^\pm}^{1L}} < 0.1\,, \tag{3.19}$$

with the ratios estimated by eqs. (3.17). We find that all of the 5000 scanned data points satisfy the first relation above, while 609 do not satisfy the second relation. In all the following results we retain only the scanned data points that satisfy eqs. (3.19).

The distribution of viable data points of the bNMWT allowed parameter space in the (S, T) plane is shown in figure 2. The 90% Confidence Level (CL) allowed region is shaded in green while the viable data points featuring $m_H^2 > 0$ ($m_H^2 < 0$) are plotted in black (grey). We make this distinction because for positive m_H^2 the SM Higgs sector alone would not break EW symmetry, and therefore EW symmetry breaking is generated through bosonic TC interactions. The black dots are, thus, relevant for bNMWT while the grey ones refer more generically to the Type-I 2HDM. It is clear that the viable region in S and T accessible by bNMWT is very limited.

JHEP01(2014)041

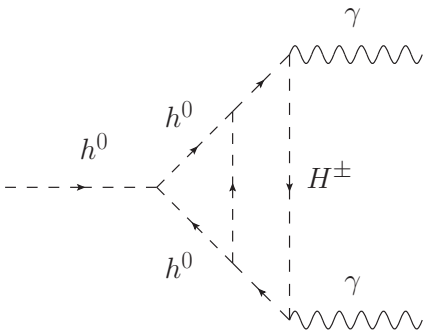

Figure 1. Feynman diagram for the 2 loop contribution of virtual scalars to the h^0 decay to diphoton.

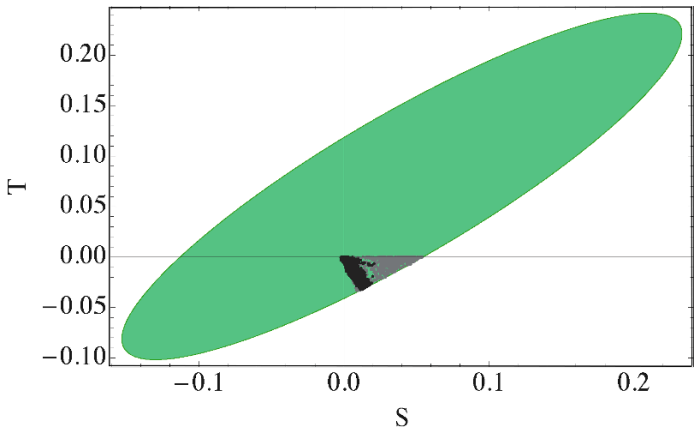

Figure 2. 90%CL viable region (in green) of the precision EW parameters S and T: in black are the values relevant for bNMWT, while those in grey refer generically to Type-I 2HDM.

In figure 3 we plot the viable data points in the (a_S, a_f) and (a_S, a_V) planes, respectively, together with the 68% (green), 90% (blue), and 95% (yellow) CL regions obtained in the previous section: these plots represent a slice of the a_f, a_V, and a_S parameter space passing through the optimal point (blue star) given in eq. (2.13). There is a perfectly specular viable region, which we do not show here, intersecting another χ^2 global minimum point, obtained by flipping the signs of a_V, a_f, and a_S in eq. (2.13). In figure 3, left panel, the upper viable region, containing the best fit point, obtains the observed slight enhancement of the Higgs diphoton decay rate exclusively by the charged scalar contribution which interferes constructively with the W boson contribution. This results from a rather large linear coupling of h^0 to $S^\pm$. In the lower viable region, the slight enhancement of the Higgs diphoton decay rate is entirely due to the SM fermions which couple to h^0 with the same sign as $W^\pm$ and, therefore, give constructive interference, while the scalar interferes destructively to balance an otherwise excessive enhancement of the decay rate to two photons. The same comments apply to the viable regions presented in figure 3, right panel.

The bNMWT data points are closely clustered around the SM values. This was somewhat expected, because of the small mixing of the two neutral Higgs fields for a heavy

JHEP01(2014)041

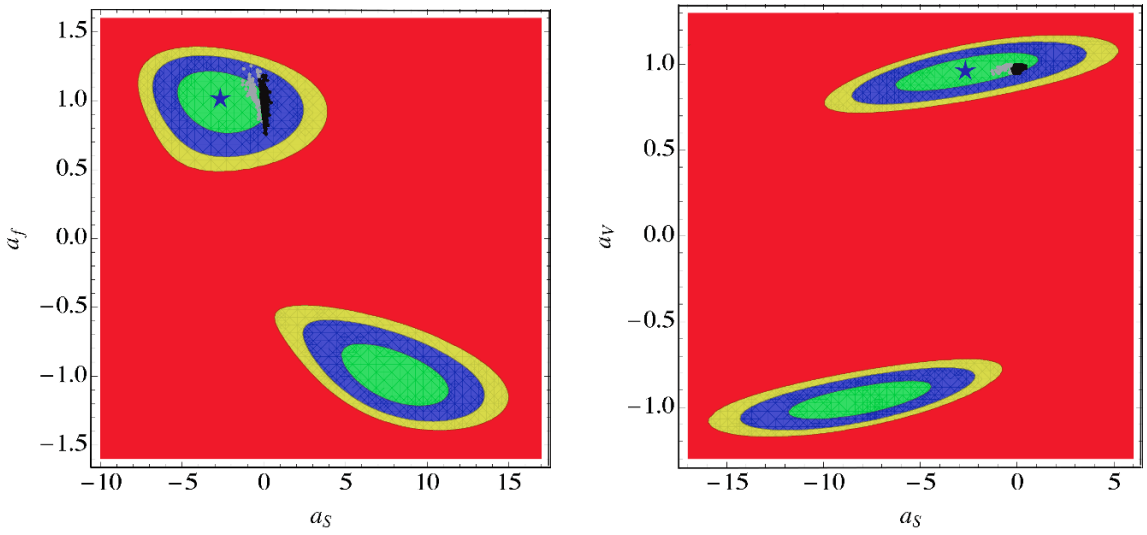

Figure 3. Viable data points in the (a_S, a_f) (left pane) and (a_S, a_V) (right pane) planes, together with the 68% (green), 90% (blue), and 95% (yellow) CL region: in black are the values relevant for bNMWT while those in grey refer generically to Type-I 2HDM. The blue stars mark the optimal coupling coefficients on the respective planes intersecting the optimal point with $a_{V'} = 0$.

H mass. The choice of a heavy masses for the new states is naively dictated by strong dynamics, which in the scaled up QCD case would predict masses of $O(\Lambda_{TC}) \approx$ TeV.

Finally, in figure 4 we show the bNMWT data points in the (a_V, a_f) plane that passes through the SM point $(a_S = a_f = a_V = 0)$ to which they approximately belong. In bNMWT the Higgs-vector boson coupling is always reduced compared to its SM value, as shown in figure 4, while the experiment favors an enhancement of the same coupling. While bNMWT looks generally disfavored compared to the SM, most of the scanned data points lie within the 90% CL region.

We note that figure 2 also includes bNMWT points with flipped sign of a_f, a_V, and a_S. These points belong to the plane passing through the specular optimal point, and therefore we do not include them in figures 3 and 4.

Among the scanned viable bNMWT data points featuring $m_H^2 > 0$, the one minimizing χ^2 is

$$a_V = 1.00\,,\ a_f = 0.98\,,\ a_S = 0.0\,, \qquad S = T = 0 \quad . \tag{3.20}$$

The result above is derived in the limit of heavy $H^\pm$ for the diphoton decay amplitude, eqs. (2.8). The average mass of $H^\pm$ and A for the viable data points is about 800 GeV: even for the lightest charged scalar mass, equal to 170 GeV, the change in the light Higgs decay rate to diphoton is smaller than 1%, and therefore negligible compared to the experimental uncertainty. This justifies the heavy $H^\pm$ approximation we used for for the diphoton decay amplitude, eqs. (2.8), in determining the optimal viable point given above.

To estimate the goodness of fit of the scanned data points, we have to determine the number of degrees of freedom (d.o.f.) of the bNMWT parameter space, limited by the constraints motivated by strong dynamics. Since the free variables in the bNMWT La-

JHEP01(2014)041

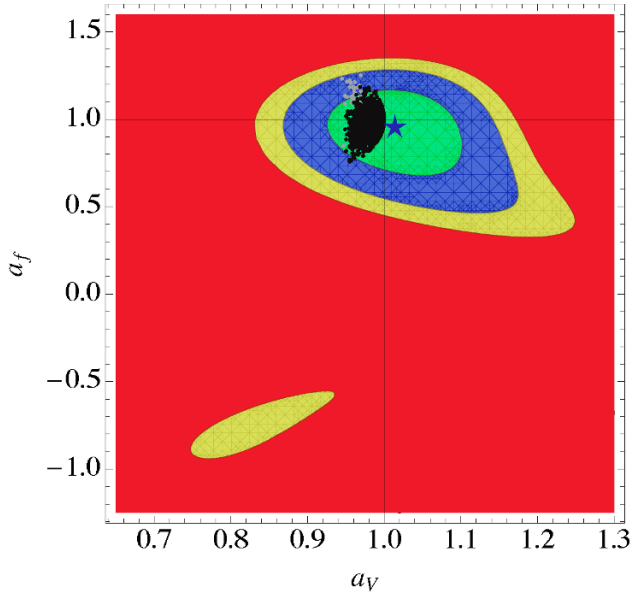

Figure 4. Viable data points in the (a_V, a_f) plane, together with the 68% (green), 90% (blue), and 95% (yellow) CL region: in black are the values relevant for bNMWT while those in grey refer generically to Type-I 2HDM. The blue star marks the optimal coupling coefficients on the (a_V, a_f) plane for $a_S = a_{V'} = 0$.

grangian in eqs. (3.2), (3.4) can be grouped in the coupling coefficients of eq. (2.2), defined in terms of the TC Lagrangian variables by eq. (3.12), one can expect the Higgs physics data presented in section 2 to allow at most for three d.o.f., plus two since we also include the EW parameters S and T in the fit. In practice, the range of values found with the scan for a_S, S, T, is very small compared to the uncertainty affecting each of those parameters. We assume, therefore, to have only two free parameter, a_f and a_V, which produce the following statistical results:

$$\chi^2_{\rm min}/\text{d.o.f.} = 0.99\,, \quad P\left(\chi^2 > \chi^2_{\rm min}\right) = 47\%\,, \quad \text{d.o.f.} = 17\,. \tag{3.21}$$

These numbers should be compared to the corresponding results in the SM, eq. (2.16), which indeed produces a better fit.

For further comparison, we also give the corresponding results for the generic 2HDM data points ($m_H^2 < 0$):

$$\begin{aligned} &a_V = 1.00\,, \qquad a_f = 0.99\,, \qquad a_S = -0.4\,, \quad S = 0.01\,, \quad T = 0\,; \\ &\chi^2_{\rm min}/\text{d.o.f.} = 0.99\,, \quad P\left(\chi^2 > \chi^2_{\rm min}\right) = 47\%\,, \quad \text{d.o.f.} = 17. \end{aligned} \tag{3.22}$$

The charged scalar for the viable data points has a mass on average equal to 2.6 TeV, with a minimum around 400 GeV. This justifies the heavy mass limit we used in determining the optimal point above.

The results obtained so far for bNMWT do not take into account the contributions to Higgs physics coming from heavy charged vector bosons, which are a staple of strong dynamics. In the next section we study this subject by introducing the relevant interaction terms in the Lagrangian and by working out the corresponding Higgs physics phenomenology.

JHEP01(2014)041

4 Extra charged vector bosons and experimental data fit

Extra vector bosons arise naturally in TC as composite resonances with a mass of the order of the strong interaction scale Λ_{TC}. Of particular interest to us here is the possibility that an extra charged vector boson, W', be responsible for the observed slight enhancement to the diphoton decay rate of the Higgs even if $m_{W'} \gg m_{h^0}$. Given the LHC constraints on the mass $m_{W'}$, equal to 2.55 TeV [48], it is safe to take the heavy W' limit, eq. (2.8), for the Higgs decay rate to $\gamma\gamma$ in eq. (2.5).

To introduce, in the effective Lagrangian, direct Higgs couplings to an extra massive vector boson which conserves gauge symmetry at the fundamental scale, we use the hidden local symmetry principle [68, 69], which has been already applied to NMWT in [40, 70]: here we just outline the main steps required to introduce composite vector bosons while conserving gauge invariance in the fundamental theory.

We begin by defining the following covariant derivatives

$$D^\mu N_L = \partial^\mu N_L + i g_L \tilde{W}^\mu N_L + i g_{TC} A_L^\mu N_L \,, \quad D^\mu N_R = \partial^\mu N_R + i g_Y \tilde{B}^\mu N_R + i g_{TC} A_R^\mu N_R \,, \tag{4.1}$$

where A_μ is the vector boson associated with the $G \equiv \mathrm{SU}(2) \times \mathrm{SU}(2)$ global symmetry of $\mathcal{L}_{TC}$, which we have gauged above, and N_L (N_R) is a scalar field in the fundamental of $\mathrm{SU}(2)_L$ ($\mathrm{U}(1)_Y$) and antifundamental of G. From the equations above, we can define a new vector field and its transformation under the full gauged symmetry by

$$\mathrm{Tr}\left[N_L N_L^\dagger\right] P_L^\mu = \frac{D^\mu N_L N_L^\dagger - N_L D^\mu N_L^\dagger}{i g_{TC}} \,, \quad P_L^\mu \to u_L P_L^\mu u_L^\dagger \,, \tag{4.2}$$

where u_L is a unitary transformation operator of SU(2). The definition and transformation law of P_R are obtained simply by replacing L with R in eq. (4.2). The only dimension four, gauge invariant P^μ non-derivative coupling terms to M are the following

$$\mathcal{L}_{M-P} = -g_{TC}^2 r_2 \mathrm{Tr}\left[P_{L\mu} M' P_R^\mu M'^\dagger\right] + \frac{g_{TC}^2 r_1}{4} \mathrm{Tr}\left[P_{L\mu}^2 + P_{R\mu}^2\right] \mathrm{Tr}\left[M' M'^\dagger\right] \,, \tag{4.3}$$

where M' is the matrix representation of the EW doublet M. We do not consider derivative couplings of the composite vectors to minimize the contributions to the oblique corrections, in particular to the S-parameter. Assigning non-zero vevs for N_L and N_R, their kinetic terms generate a squared mass term for two vector boson combinations:

$$m_A^2 \mathrm{Tr}\left[C_{L\mu}^2 + C_{R\mu}^2\right] \,, \quad C_L^\mu \equiv \langle P_L^\mu \rangle = A_L^\mu - \frac{g_L}{g_{TC}} \tilde{W}^\mu \,, \quad C_R^\mu \equiv \langle P_R^\mu \rangle = A_R^\mu - \frac{g_Y}{g_{TC}} \tilde{B}^\mu \,. \tag{4.4}$$

The resulting massless eigenstates give the ordinary W^μ and B^μ vector bosons, which instead acquire mass through EW symmetry breaking. In addition, there are two vector boson triplets, one vectorial (V^μ) and the other axial (A^μ). Since their interaction terms, given by eq. (4.3) evaluated at the vev defined in eq. (4.4), respect custodial symmetry and give the same contribution to the axial-axial and vector-vector EW vector boson polarization functions [71], the total contribution of the vector bosons to the EW precision parameters is identical to the SM one, and S and T are, therefore, zero [40, 70]. Moreover

JHEP01(2014)041

the vector boson contributions to FCNC have been tested against the experimental results and shown to be phenomenologically viable [72]. To simplify our analysis we fix

$$r_2 = -r_1\,, \tag{4.5}$$

so that only $\tilde{W}^\mu$ and the vector resonance, V^μ, couple to the neutral Higgs fields. The restrictions we have made on the couplings of the composite vector mesons can be released at the expense of introducing more free parameters into the model. However, we take the restricted interactions as sufficient for exhibiting the viability of the present model, and expect that the values of the parameters we determine through our analysis will serve as a useful benchmark example of viable portion of the parameter space also for cases where additional interactions are included.

The charged vector boson mass matrix in the $(\tilde{W}, V, A)$ basis can be written in a compact form as

$$\begin{pmatrix} m_{\tilde{W}}^2 & -\frac{\epsilon m_V^2}{\sqrt{2}} & -\frac{\epsilon m_A^2}{\sqrt{2}} \\ -\frac{\epsilon m_V^2}{\sqrt{2}} & m_V^2 & 0 \\ -\frac{\epsilon m_A^2}{\sqrt{2}} & 0 & m_A^2 \end{pmatrix}, \tag{4.6}$$

with

$$m_{\tilde{W}} = \left[x^2 + \left(1+s^2\right)\epsilon^2\right] m_A^2\,, \quad m_V^2 = \left(1+2s^2\right) m_A^2\,, \tag{4.7}$$

and

$$s \equiv \frac{g_{\rm TC} f}{2m_A}\sqrt{r_1}\,, \quad x \equiv \frac{g_L v_w}{2m_A}\,, \quad \epsilon \equiv \frac{g_L}{g_{TC}}\,. \tag{4.8}$$

We now study the implications of this setup in light of the LHC and Tevatron data fit we have at our disposal.

4.1 Mixing of vector fields

Let us begin with a rather general and simple case. We require that only $\tilde{W}$, the elementary gauge field, couples to h^0, and therefore the W' coupling to the light Higgs is generated only through terms mixing $\tilde{W}$ with the composite vector fields V and A. The squared mass matrix in the gauge basis $(\tilde{W}, V, A)$ is obtained simply by setting $s = 0$ in eqs. (4.6), (4.7):

$$\begin{pmatrix} \frac{g_L^2 v_w^2}{4} + \epsilon^2 m_A^2 & -\frac{\epsilon m_A^2}{\sqrt{2}} & -\frac{\epsilon m_A^2}{\sqrt{2}} \\ -\frac{\epsilon m_A^2}{\sqrt{2}} & m_A^2 & 0 \\ -\frac{\epsilon m_A^2}{\sqrt{2}} & 0 & m_A^2 \end{pmatrix}. \tag{4.9}$$

We define the rotation to the mass eigenbasis in terms of x and ϵ, eqs. (4.8), by

$$\begin{pmatrix} \tilde{W} \\ V \\ A \end{pmatrix} = \begin{pmatrix} c_\varphi & -s_\varphi & 0 \\ \frac{s_\varphi}{\sqrt{2}} & \frac{c_\varphi}{\sqrt{2}} & -\frac{1}{\sqrt{2}} \\ \frac{s_\varphi}{\sqrt{2}} & \frac{c_\varphi}{\sqrt{2}} & \frac{1}{\sqrt{2}} \end{pmatrix} \begin{pmatrix} W \\ W' \\ W'' \end{pmatrix}, \quad c_\varphi = \frac{1}{\sqrt{2}}\sqrt{1 + \frac{1-x^2-\epsilon^2}{\sqrt{(1+x^2+\epsilon^2)^2 - 4x^2}}}\,, \tag{4.10}$$

JHEP01(2014)041

with corresponding eigenvalues

$$m^2_{W,W'} = \frac{1}{2}\left[1 + x^2 + \epsilon^2 \mp \sqrt{(1 + x^2 + \epsilon^2)^2 - 4x^2}\right] m_A^2 \,, \quad m^2_{W''} = m_A^2 \,. \tag{4.11}$$

The mixing matrix in eq. (4.10) shows that only W and W' contribute to the gauge field $\tilde{W}$.

We checked that the Fermi coupling, G_F, determined by evaluating the amplitude for the muon decay ($\mu^- \to \nu_\mu \bar{\nu}_e e^-$), respects the usual relation

$$\sqrt{2} G_F = v_w^{-2} = (246\,\text{GeV})^{-2} \,. \tag{4.12}$$

The vector coupling coefficient a_V is suppressed, compared to the result in eq. (3.12), because of mixing:

$$a_V = c^2_{\varphi'} s_{\beta-\alpha} \,, \quad a_{V'} = s^2_{\varphi'} s_{\beta-\alpha} \,, \tag{4.13}$$

with

$$c^2_{\varphi'} = \frac{g_L^2 v_w^2}{4 m_W^2} c^2_\varphi = \frac{2x^2\epsilon^2}{(1 + x^2 + \epsilon^2)^2 - 4x^2 - (1 - x^2 + \epsilon^2)\sqrt{(1 + x^2 + \epsilon^2)^2 - 4x^2}} \,. \tag{4.14}$$

The W'' coupling to h^0 is zero instead because we set $r_2 = -r_1$ in eq. (4.3). Finally, the fermion and scalar coupling coefficients in eq. (3.12) remain unchanged.

The lower limit on the mass of a sequential[3] W' from direct searches at ATLAS [48], equal to 2.55 TeV at 95%CL, can be readily applied to the case above by properly rescaling the lower limit:

$$\Gamma_{W' \to l\nu} = \frac{g^2_{W'} m_{W'}}{48\pi} \quad \Rightarrow \quad m_{W'} > (2.55\text{TeV}) \left(\frac{g_{W'}}{g_W}\right)^2 \,, \; \frac{g_{W'}}{g_W} = -s_{\varphi'} \frac{m_{W'}}{m_W} \,, \tag{4.15}$$

with $s_{\varphi'}, m_{W'}, m_W$ defined in terms of x, ϵ, and m_A by eqs. (4.14), (4.11). By plotting the experimentally viable region defined by eqs. (4.15) on the x and ϵ plane, we find the maximum allowed value of $\epsilon = 0.36$ (at the 95%CL), reached at $x = 0$ (equivalent to the limit of large m_A).

In strong dynamics the value of m_A is expected to be of $O(\text{TeV})$, which determines x to be of $O(10^{-2})$. In general this needs not to be the case, as larger values of x for small ϵ are allowed by the experiment. On the other hand we are interested primarily in testing bNMWT, and therefore in the following we will limit our analysis by assuming $x \ll 1$. This choice, moreover, guarantees that the W couplings do not change dramatically. Also, ϵ is expected to be small because of eqs. (4.8) and the fact that $g_{TC} \gg g_L$. An expansion in both ϵ and x therefore produces

$$a_V = s_{\beta-\alpha}\left(1 - x^2\epsilon^2\right) + O\left(x^n \epsilon^{5-n}\right) \,, \quad a_{V'} = s_{\beta-\alpha} x^2 \epsilon^2 + O\left(x^n \epsilon^{5-n}\right) \,, \quad n = 0, \ldots, 5 \,. \tag{4.16}$$

In this limit the effect of mixing on the W' and W couplings is negligible. Moreover, because the sum of a_V and $a_{V'}$ is independent of ϵ, so is the Higgs decay rate to two photons.

[3] A sequential W' has the same couplings as the SM W.

JHEP01(2014)041

Therefore, the optimal values for bNMWT with $m_A = 1\,\text{TeV}$, $\epsilon < 0.36$, and $m_H^2 > 0$ ($m_H^2 < 0$) correspond to the ones with no mixing ($\epsilon = 0$), presented in eqs. (3.20) (eqs. (3.22)). In

In the next subsection we study the phenomenologically more appealing scenario in which the composite vector fields feature a direct coupling to neutral Higgs fields.

4.2 Direct Higgs coupling to W' and W''

Next we want to study the effects of a direct Higgs coupling to the composite vector field V, and consider $s \neq 0$. In this case, the charged vector boson mass matrix in the $(\tilde{W}, V, A)$ basis is given by eq. (4.6). The mass eigenvalues are lengthy cubic roots. These can be expanded in x and ϵ, which in TC are both expected to be small:

$$\begin{aligned} m_W^2 &\cong m_A^2 x^2 \left[1 - \epsilon^2\right] , \quad m_{W''}^2 \cong m_A^2 \left[1 + \frac{1}{2}\left(1 + x^2\right)\epsilon^2 - \frac{1}{8}\left(2 + \frac{1}{s^2}\right)\epsilon^4\right] , \\ m_{W'}^2 &\cong m_A^2 \left[1 + 2s^2 + \frac{1}{2}\left(1 + 2s^2 + x^2\right)\epsilon^2 + \frac{1}{8}\left(2 + \frac{1}{s^2}\right)\epsilon^4\right] , \end{aligned} \tag{4.17}$$

where contributions of $O(x^n \epsilon^{5-n})$ are neglected, with $n = 0, \ldots, 5$. The $\tilde{W}$ and V coupling terms to the light Higgs can be derived from the mass matrix by taking its derivative with respect to v_w and introducing a factor ζ to take into account the rotation of M to the mass eigenbasis:

$$\mathcal{L} \supset \frac{2m_A^2}{v_w} s_{\beta-\alpha} \left[\left(x^2 + \zeta s^2 \epsilon^2\right)\tilde{W}\tilde{W} + 2\zeta s^2 VV - 2\sqrt{2}\zeta s^2 \epsilon \tilde{W} V\right] h^0 , \quad \zeta = s_{\beta-\alpha}^{-1} \frac{c_{\alpha+\rho}}{s_{\beta+\rho}} . \tag{4.18}$$

The vector boson coupling coefficients get an enhancement factor because of the s coupling:

$$a_V = \eta_W s_{\beta-\alpha} , \quad a_{V'} = \left(\eta_{W'} + \eta_{W''}\right) s_{\beta-\alpha} , \tag{4.19}$$

where

$$\begin{aligned} \eta_W &\cong 1 - \frac{\left[1 + s^2\left(3 - \zeta\right) + 2s^4\right] x^2 \epsilon^2}{\left(1 + 2s^2\right)^2} , \quad \eta_{W'} \cong \frac{2\zeta s^2}{1 + 2s^2} + \frac{\left[1 + 2s^2\left(1 - \zeta\right)\right] x^2 \epsilon^2}{2\left(1 + 2s^2\right)^2} - \frac{\zeta \epsilon^4}{8s^2} , \\ \eta_{W''} &\cong \frac{x^2 \epsilon^2}{2} + \frac{\zeta \epsilon^4}{8s^2} , \end{aligned} \tag{4.20}$$

at $O(x^n \epsilon^{5-n})$, with $n = 0, \ldots, 5$. We collected together the W' and W'' contributions to the Higgs decay to diphoton by summing up their respective coupling coefficients in eq. (4.19). It is interesting to notice that, at all orders in x:

$$\eta_W + \eta_{W'} + \eta_{W''} = 1 + \frac{2\zeta s^2}{1 + 2s^2} + O(\epsilon^5) . \tag{4.21}$$

The fermion and scalar coefficients are still determined by eqs. (3.12). We obtain the optimal value of s by performing the global fit in the limit of negligible vector mixing ($\epsilon = 0$) and decoupled neutral heavy Higgs:

$$a_f = a_V = 1 , \quad a_S = 0 , \quad a_{V'} = \frac{2s^2}{1 + 2s^2} , \quad \Rightarrow \quad s = 0.21^{+0.18}_{-0.21} . \tag{4.22}$$

JHEP01(2014)041

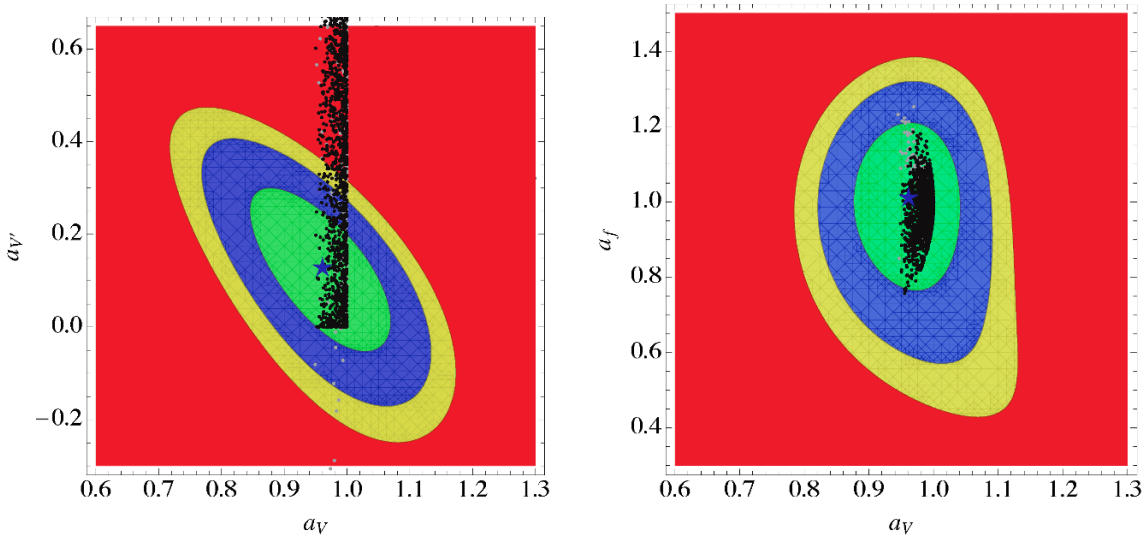

Figure 5. Viable data points in the $(a_V, a_{V'})$ and (a_V, a_f) planes, together with the 68% (green), 90% (blue), and 95% (yellow) CL region: in black are the values relevant for bNMWT while those in grey refer generically to Type-I 2HDM with the addition of two charged vector bosons. The blue stars mark the optimal coupling coefficients on the respective planes intersecting the optimal point with $a_S = 0$.

We use the same set of viable points scanned over the bNMWT parameter space with no W' and W'', and re-calculate the coupling coefficients a_V and $a_{V'}$ at each data point for random values of s and ϵ, with $0 \leq s \leq 1$ and $0 \leq \epsilon \leq 0.1$, and $m_A = 1\,\text{TeV}$. We plot the resulting bNMWT data points together with the experimentally favored regions in the $(a_V, a_{V'})$ and (a_V, a_f) planes in figure 5, and in the $(a_{V'}, a_f)$ plane in figure 6, respectively, all passing through the optimal data point defined in eq. (2.13). The plots are again limited to the positive a_V half-plane. For $m_H^2 < 0$ the mixing factor ζ, eq. (4.18), can be negative, which makes $a_{V'}$ flip sign, compared to a_V, because of eqs. (4.20). Already by visual inspection, it is clear that the s coupling allows bNMWT to cover a large portion of the 68% CL favored region. We verified that all the three parameters $a_f, a_{V'}$, and (to a lesser degree) a_V are free (meaning that they are little correlated and with a range of values comparable to the error affecting the optimal values in eq. (2.13)), which was expected since we introduced the new parameter s. In this case the bNMWT data point minimizing χ^2 for $m_H^2 > 0$ is

$$\begin{aligned} a_V = 1.00\,, \qquad a_f = 1.00\,, \qquad a_{V'} = 0.09\,, \quad a_S = 0.0\,, \quad S = T = 0.00\,; \\ \chi^2_{\text{min}}/\text{d.o.f.} = 1.00\,, \quad P\left(\chi^2 > \chi^2_{\text{min}}\right) = 45\%\,, \quad \text{d.o.f.} = 16, \end{aligned} \tag{4.23}$$

while for $m_H^2 < 0$ we find

$$\begin{aligned} a_V = 1.00\,, \qquad a_f = 0.99\,, \qquad a_{V'} = 0.05\,, \quad a_S = -0.4\,, \quad S = T = 0.00\,; \\ \chi^2_{\text{min}}/\text{d.o.f.} = 1.02\,, \quad P\left(\chi^2 > \chi^2_{\text{min}}\right) = 43\%\,, \quad \text{d.o.f.} = 16. \end{aligned} \tag{4.24}$$

The W' and W'' masses corresponding to the optimal points above are equal to about 1 TeV. In the scanned slice of parameter space the upper limit on vector boson masses

JHEP01(2014)041

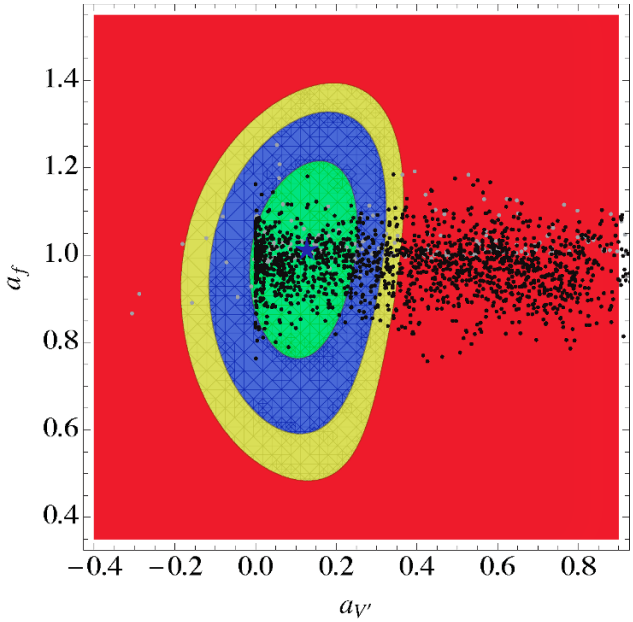

Figure 6. Viable data points in the $(a_{V'}, a_f)$ plane, together with the 68% (green), 90% (blue), and 95% (yellow) CL region: in black are the values relevant for bNMWT while those in grey refer generically to Type-I 2HDM with the addition of two charged vector bosons. The blue star marks the optimal coupling coefficients on the $(a_{V'}, a_f)$ plane for optimal a_V and with $a_S = 0$.

determined by eqs. (4.17), (4.22) corresponds to 1.15 TeV, which is consistent with the Λ_{TC} cutoff implied by the effective Lagrangian defined in eqs. (3.4), (4.3). We estimated the two loop contributions of virtual heavy vector bosons to the Higgs decay to diphoton, and found them negligible in comparison to two loop contributions of virtual scalars. This result together with the fact that the scanned data points satisfy eqs. (3.19) ensures that higher order contributions are negligible in first appoximation.

The two cases in eqs. (4.23), (4.24), respectively, are equally favored by the experiment and both feature a probability greater than the one for the general fit, eq. (2.13), which does not include the S and T EW parameters (and therefore has two less d.o.f.) but gives a similar value of $\chi^2_{\rm min}$. The value of $\chi^2_{\rm min}$ corresponding to the data points above is smaller than that obtained without composite vector bosons, eqs. (3.21), (3.22), though the additional free parameter counterbalances this gain. As a last remark, we note that $a_{V'}$ is rather unconstrained by the chosen set of observables, and so a broader set of observables related to W' physics would be necessary to further test the viability of bNMWT.

5 Conclusions and outlook

In this paper we have considered quantitatively how much the coefficients of Higgs couplings to electroweak gauge bosons (a_V) and fermions (a_f) as well as to possible extra scalars (a_S) can deviate from their corresponding values in the Standard Model ($a_V = a_f = 1$, $a_S = 0$) in light of the current LHC and Tevatron data. We then considered a bosonic technicolor model, bNMWT [41], and studied its viability by performing a scan on the parameter space

JHEP01(2014)041

which implements the direct constraints on the mass spectrum as well as the constraints from precision EW data (in terms of the S and T parameters). The scalar sector of the bosonic technicolor model we considered can be more generally viewed as a type-I 2HDM.

The essential consequence of underlying strong dynamics is the existence of new vector resonances in the particle spectrum. We implemented these new states in an effective Lagrangian to study their effects. We considered in detail the implications of the effective Lagrangian on the couplings of the Higgs boson to the physical W and Z bosons as well as to fermions. Then, we studied first the simple case of minimal coupling to the SM fields, which amounts to considering only the mixing of the two new triplets of vector bosons and the $\mathrm{SU}(2)_L$ gauge fields without direct interaction between the composite vector bosons and SM fields. In this simple scenario we determined the 95%CL upper bound on the amount of mixing allowed by experimental data. We showed that this generic scenario in bNMWT cannot be resolved by the current data.

Finally we illustrated the possible effects of the direct coupling between composite vector bosons and neutral scalar fields within our effective Lagrangian scheme. We showed that the direct coupling produces a goodness of fit of the bNMWT predictions to the current experimental data comparable to that of the SM, though somewhat lower (P-value for the SM: 60% vs. 45% for bNMWT). Based on the results we have derived in this paper, one can proceed to evaluate the cross sections for the production of composite vectors, for example through Drell-Yan processes or quark-antiquark annihilation with one or three leptons plus missing energy in the final state. Searches for such particles at LHC would provide further constraints on the model or could lead to new major discoveries and help decipher the physics underlying the electroweak sector of the SM.

Acknowledgments

The support from Finnish Cultural Foundation, Central Finland Regional fund is gratefully acknowledged.

A Two Higgs doublet model potential

Let us write our bosonic technicolor Lagrangian explicitly as a two-Higgs doublet model (2HDM). The starting point is given by eqs. (3.4), (3.5). The kinetic mixing term in eq. (3.4) is rotated away and the model canonically normalized by eq.(3.9). Applying one more rotation we can express the SM Yukawa couplings in the following form

$$\mathcal{L}_{\mathrm{Yuk}} = (y_u)_{ij} K H_2 \bar{Q}_i U_j + (y_d)_{ij} K H_2^\dagger \bar{Q}_i D_j + (y_\ell)_{ij} K H_2^\dagger \bar{L}_i E_j + \mathrm{h.c.}\,, \quad K = \left(1 - c_3^2 y_{TC}^2\right)^{-\frac{1}{2}}\,, \tag{A.1}$$

where the full transformation is given by

$$H = K H_2\,, \quad M = H_1 - c_3 y_{TC} K H_2\,. \tag{A.2}$$

As eq. (A.1) shows, only one of the two Higgses (by convention H_2) couples to SM fermions, which ensures that there are no tree-level contributions to Flavor Changing Neutral Currents (FCNC): such a model in literature has been referred to as Type-I 2HDM [42].

JHEP01(2014)041

On the other hand, the most general renormalizable Higgs potential of a 2HDM can be written as

$$
\begin{aligned}
V = {} & m_1^2 H_1^\dagger H_1 + m_2^2 H_2^\dagger H_2 - m_{12}^2 \left(H_1^\dagger H_2 + H_2^\dagger H_1 \right) + \frac{\lambda_1}{2} (H_1^\dagger H_1)^2 + \frac{\lambda_2}{2} (H_2^\dagger H_2)^2 \\
& + \lambda_3 (H_1^\dagger H_1)(H_2^\dagger H_2) + \lambda_4 (H_2^\dagger H_1)(H_1^\dagger H_2) + \left[\frac{\lambda_5}{2} (H_1^\dagger H_2)^2 \right. \\
& \left. - \lambda_6 (H_2^\dagger H_1)(H_1^\dagger H_1) - \lambda_7 (H_2^\dagger H_1)(H_2^\dagger H_2) + h.c. \right] .
\end{aligned}
\tag{A.3}
$$

The coefficients in eq. (A.3) can be expressed in terms of those in the potential $V(M, H)$, in the notation of [41], by:

$$
\begin{aligned}
& m_1^2 = m_M^2 \,, \;\; m_2^2 = \left[m_H^2 + \left(2 f^2 c_1 + m_M^2 c_3 \right) c_3 y_{TC}^2 \right] K^2 \,, \;\; m_{12}^2 = \left(f^2 c_1 + m_M^2 c_3 \right) y_{TC} K \,, \\
& \lambda_1 = \frac{1}{3} \lambda_M \,, \;\; \lambda_2 = \frac{1}{3} \left(2 c_2 c_3^3 y_{TC}^4 + \lambda_H + 2 c_3 c_4 y_{TC}^2 \lambda_H + c_3^4 y_{TC}^4 \lambda_M \right) K^4 \,, \\
& \lambda_3 = \lambda_4 = \lambda_5 = \frac{1}{6} \left(c_2 + c_3 \lambda_M \right) c_3 y_{TC}^2 K^2 \,, \\
& \lambda_6 = \frac{1}{6} \left(c_2 + 2 c_3 \lambda_M \right) y_{TC} K \,, \;\; \lambda_7 = \frac{1}{6} \left[c_4 \lambda_H + c_3^2 y_{TC}^2 \left(3 c_2 + 2 c_3 \lambda_M \right) \right] y_{TC} K^3 \,,
\end{aligned}
\tag{A.4}
$$

The Higgs fields in eq. (A.3) are expressed in terms of the real degrees of freedom by

$$
H_i = \begin{pmatrix} H_i^+ \\ \frac{1}{\sqrt{2}} (v_i + h_i + i \phi_i) \end{pmatrix} \,, \quad i = 1, 2 \; ; \tan \beta' \equiv \frac{v_1}{v_2} \,. \tag{A.5}
$$

The Goldstone boson $G^\pm$ (G^0) provides the longitudinal components of the $W^\pm$ (Z^0) boson, while h^0, H^0, A^0, and $H^\pm$ are the neutral scalars, pseudoscalar, and charged scalar mass eigenstates, respectively:

$$
\begin{aligned}
& \begin{pmatrix} h^0 \\ H^0 \end{pmatrix} = \begin{pmatrix} c_{\alpha'} & -s_{\alpha'} \\ s_{\alpha'} & c_{\alpha'} \end{pmatrix} \begin{pmatrix} h_1 \\ h_2 \end{pmatrix} \,, \;\; \begin{pmatrix} G^0 \\ A^0 \end{pmatrix} = \begin{pmatrix} s_{\beta'} & c_{\beta'} \\ c_{\beta'} & -s_{\beta'} \end{pmatrix} \begin{pmatrix} \phi_1 \\ \phi_2 \end{pmatrix} \,, \\
& \begin{pmatrix} G^\pm \\ H^\pm \end{pmatrix} = \begin{pmatrix} s_{\beta'} & c_{\beta'} \\ c_{\beta'} & -s_{\beta'} \end{pmatrix} \begin{pmatrix} H_1^\pm \\ H_2^\pm \end{pmatrix} \,.
\end{aligned}
\tag{A.6}
$$

The angles α', β' differ from α, β only because of the extra rotation in eq.(A.2) that makes only H_2 couple to SM fermions.

References

[1] A. Azatov, R. Contino and J. Galloway, *Model-independent bounds on a light Higgs*, *JHEP* **04** (2012) 127 [*Erratum ibid.* **04** (2013) 140] [arXiv:1202.3415] [INSPIRE].

JHEP01(2014)041

[2] D. Carmi, A. Falkowski, E. Kuflik and T. Volansky, *Interpreting LHC Higgs results from natural new physics perspective*, *JHEP* **07** (2012) 136 [arXiv:1202.3144] [INSPIRE].

[3] J. Espinosa, C. Grojean, M. Muhlleitner and M. Trott, *Fingerprinting Higgs suspects at the LHC*, *JHEP* **05** (2012) 097 [arXiv:1202.3697] [INSPIRE].

[4] P.P. Giardino, K. Kannike, M. Raidal and A. Strumia, *Reconstructing Higgs boson properties from the LHC and Tevatron data*, *JHEP* **06** (2012) 117 [arXiv:1203.4254] [INSPIRE].

[5] M. Carena, I. Low and C.E. Wagner, *Implications of a modified Higgs to diphoton decay width*, *JHEP* **08** (2012) 060 [arXiv:1206.1082] [INSPIRE].

[6] T. Corbett, O. Eboli, J. Gonzalez-Fraile and M. Gonzalez-Garcia, *Constraining anomalous Higgs interactions*, *Phys. Rev.* **D 86** (2012) 075013 [arXiv:1207.1344] [INSPIRE].

[7] P.P. Giardino, K. Kannike, M. Raidal and A. Strumia, *Is the resonance at* 125 *GeV the Higgs boson?*, *Phys. Lett.* **B 718** (2012) 469 [arXiv:1207.1347] [INSPIRE].

[8] J. Ellis and T. You, *Global analysis of the Higgs candidate with mass* $\sim$ 125 *GeV*, *JHEP* **09** (2012) 123 [arXiv:1207.1693] [INSPIRE].

[9] D. Carmi, A. Falkowski, E. Kuflik, T. Volansky and J. Zupan, *Higgs after the discovery: a status report*, *JHEP* **10** (2012) 196 [arXiv:1207.1718] [INSPIRE].

[10] S. Banerjee, S. Mukhopadhyay and B. Mukhopadhyaya, *New Higgs interactions and recent data from the LHC and the Tevatron*, *JHEP* **10** (2012) 062 [arXiv:1207.3588] [INSPIRE].

[11] N. Arkani-Hamed, K. Blum, R.T. D'Agnolo and J. Fan, 2 : 1 *for naturalness at the LHC?*, *JHEP* **01** (2013) 149 [arXiv:1207.4482] [INSPIRE].

[12] F. Bonnet, T. Ota, M. Rauch and W. Winter, *Interpretation of precision tests in the Higgs sector in terms of physics beyond the Standard Model*, *Phys. Rev.* **D 86** (2012) 093014 [arXiv:1207.4599] [INSPIRE].

[13] T. Corbett, O. Eboli, J. Gonzalez-Fraile and M. Gonzalez-Garcia, *Robust determination of the Higgs couplings: power to the data*, *Phys. Rev.* **D 87** (2013) 015022 [arXiv:1211.4580] [INSPIRE].

[14] ATLAS collaboration, *Measurements of the properties of the Higgs-like boson in the two photon decay channel with the ATLAS detector using* 25 fb^{-1} *of proton-proton collision data*, ATLAS-CONF-2013-012, CERN, Geneva Switzerland (2013).

[15] CMS collaboration, *Updated measurements of the Higgs boson at* 125 *GeV in the two photon decay channel*, CMS-PAS-HIG-13-001, CERN, Geneva Switzerland (2013).

[16] Tevatron New Physics Higgs Working Group, CDF and D0 collaborations, *Updated combination of CDF and D0 searches for Standard Model Higgs boson production with up to* 10.0 fb^{-1} *of data*, arXiv:1207.0449 [INSPIRE].

[17] CDF and D0 collaborations, T. Aaltonen et al., *Higgs boson studies at the Tevatron*, *Phys. Rev.* **D 88** (2013) 052014 [arXiv:1303.6346] [INSPIRE].

[18] M. Carena, S. Gori, N.R. Shah, C.E. Wagner and L.-T. Wang, *Light stau phenomenology and the Higgs* $\gamma\gamma$ *rate*, *JHEP* **07** (2012) 175 [arXiv:1205.5842] [INSPIRE].

[19] A. Arbey, M. Battaglia, A. Djouadi and F. Mahmoudi, *The Higgs sector of the phenomenological MSSM in the light of the Higgs boson discovery*, *JHEP* **09** (2012) 107 [arXiv:1207.1348] [INSPIRE].

JHEP01(2014)041

[20] J.-J. Cao, Z.-X. Heng, J.M. Yang, Y.-M. Zhang and J.-Y. Zhu, *A SM-like Higgs near 125 GeV in low energy SUSY: a comparative study for MSSM and NMSSM*, *JHEP* **03** (2012) 086 [arXiv:1202.5821] [INSPIRE].

[21] N.D. Christensen, T. Han and S. Su, *MSSM Higgs bosons at the LHC*, *Phys. Rev.* **D 85** (2012) 115018 [arXiv:1203.3207] [INSPIRE].

[22] J.F. Gunion, Y. Jiang and S. Kraml, *The constrained NMSSM and Higgs near 125 GeV*, *Phys. Lett.* **B 710** (2012) 454 [arXiv:1201.0982] [INSPIRE].

[23] S. King, M. Muhlleitner and R. Nevzorov, *NMSSM Higgs benchmarks near 125 GeV*, *Nucl. Phys.* **B 860** (2012) 207 [arXiv:1201.2671] [INSPIRE].

[24] J. Ellis and K.A. Olive, *Revisiting the Higgs mass and dark matter in the CMSSM*, *Eur. Phys. J.* **C 72** (2012) 2005 [arXiv:1202.3262] [INSPIRE].

[25] R. Contino, D. Marzocca, D. Pappadopulo and R. Rattazzi, *On the effect of resonances in composite Higgs phenomenology*, *JHEP* **10** (2011) 081 [arXiv:1109.1570] [INSPIRE].

[26] J. Espinosa, C. Grojean and M. Muhlleitner, *Composite Higgs under LHC experimental scrutiny*, *EPJ Web Conf.* **28** (2012) 08004 [arXiv:1202.1286] [INSPIRE].

[27] N. Haba, K. Kaneta, Y. Mimura and R. Takahashi, *Enhancement of Higgs to diphoton decay width in non-perturbative Higgs model*, *Phys. Lett.* **B 718** (2013) 1441 [arXiv:1207.5102] [INSPIRE].

[28] M.T. Frandsen and F. Sannino, *Discovering a light scalar or pseudoscalar at the Large Hadron Collider*, arXiv:1203.3988 [INSPIRE].

[29] C. Du et al., *Discovering new gauge bosons of electroweak symmetry breaking at LHC-8*, *Phys. Rev.* **D 86** (2012) 095011 [arXiv:1206.6022] [INSPIRE].

[30] T. Abe, N. Chen and H.-J. He, *LHC Higgs signatures from extended electroweak gauge symmetry*, *JHEP* **01** (2013) 082 [arXiv:1207.4103] [INSPIRE].

[31] J.R. Andersen, T. Hapola and F. Sannino, *W' and Z' limits for minimal walking technicolor*, *Phys. Rev.* **D 85** (2012) 055017 [arXiv:1105.1433] [INSPIRE].

[32] S. Dimopoulos and L. Susskind, *Mass without scalars*, *Nucl. Phys.* **B 155** (1979) 237 [INSPIRE].

[33] E. Farhi and L. Susskind, *Technicolor*, *Phys. Rept.* **74** (1981) 277 [INSPIRE].

[34] N. Arkani-Hamed, A. Cohen, E. Katz and A. Nelson, *The littlest Higgs*, *JHEP* **07** (2002) 034 [hep-ph/0206021] [INSPIRE].

[35] N. Arkani-Hamed et al., *The minimal moose for a little Higgs*, *JHEP* **08** (2002) 021 [hep-ph/0206020] [INSPIRE].

[36] L. Randall and R. Sundrum, *A large mass hierarchy from a small extra dimension*, *Phys. Rev. Lett.* **83** (1999) 3370 [hep-ph/9905221] [INSPIRE].

[37] N. Arkani-Hamed, S. Dimopoulos and G. Dvali, *The hierarchy problem and new dimensions at a millimeter*, *Phys. Lett.* **B 429** (1998) 263 [hep-ph/9803315] [INSPIRE].

[38] F. Sannino and K. Tuominen, *Orientifold theory dynamics and symmetry breaking*, *Phys. Rev.* **D 71** (2005) 051901 [hep-ph/0405209] [INSPIRE].

JHEP01(2014)041

[39] D.D. Dietrich, F. Sannino and K. Tuominen, *Light composite Higgs from higher representations versus electroweak precision measurements: predictions for CERN LHC*, *Phys. Rev.* **D 72** (2005) 055001 [hep-ph/0505059] [INSPIRE].

[40] A. Belyaev et al., *Technicolor walks at the LHC*, *Phys. Rev.* **D 79** (2009) 035006 [arXiv:0809.0793] [INSPIRE].

[41] M. Antola, M. Heikinheimo, F. Sannino and K. Tuominen, *Unnatural origin of fermion masses for technicolor*, *JHEP* **03** (2010) 050 [arXiv:0910.3681] [INSPIRE].

[42] G. Branco et al., *Theory and phenomenology of two-Higgs-doublet models*, *Phys. Rept.* **516** (2012) 1 [arXiv:1106.0034] [INSPIRE].

[43] ATLAS collaboration, *Measurements of Higgs boson production and couplings in diboson final states with the ATLAS detector at the LHC*, *Phys. Lett.* **B 726** (2013) 88 [arXiv:1307.1427] [INSPIRE].

[44] ATLAS collaboration, *Search for the bb decay of the Standard Model Higgs boson in associated W/ZH production with the ATLAS detector*, ATLAS-CONF-2013-079, CERN, Geneva Switzerland (2013).

[45] CMS collaboration, M. Vidal, *Higgs physics at the CMS*, presentation at *ICNFP* 2013, Kolymbari Crete Greece August 28–September 5 2013.

[46] ATLAS collaboration, *Search for the Standard Model Higgs boson in $H \to \tau\tau$ decays in proton-proton collisions with the ATLAS detector*, ATLAS-CONF-2012-160, CERN, Geneva Switzerland (2012).

[47] J.F. Gunion, H.E. Haber, G.L. Kane and S. Dawson, *The Higgs hunter's guide*, *Front. Phys.* **80** (2000) 1 [INSPIRE].

[48] ATLAS collaboration, *ATLAS search for a heavy gauge boson decaying to a charged lepton and a neutrino in $4.7\,\text{fb}^{-1}$ of pp collisions at $\sqrt{s} = 7$ TeV*, ATLAS-CONF-2012-086, CERN, Geneva Switzerland (2012).

[49] ALEPH collaboration, A. Heister et al., *Search for charged Higgs bosons in e^+e^- collisions at energies up to $\sqrt{s} = 209$ GeV*, *Phys. Lett.* **B 543** (2002) 1 [hep-ex/0207054] [INSPIRE].

[50] LHC Higgs Cross section Working Group collaboration, S. Dittmaier et al., *Handbook of LHC Higgs cross sections: 1. Inclusive observables*, arXiv:1101.0593 [INSPIRE].

[51] LHC Higgs Cross section Working Group collaboration, S. Dittmaier et al., *Handbook of LHC Higgs cross sections: 2. Differential distributions*, arXiv:1201.3084 [INSPIRE].

[52] M.E. Peskin and T. Takeuchi, *Estimation of oblique electroweak corrections*, *Phys. Rev.* **D 46** (1992) 381 [INSPIRE].

[53] H.-J. He, N. Polonsky and S.-F. Su, *Extra families, Higgs spectrum and oblique corrections*, *Phys. Rev.* **D 64** (2001) 053004 [hep-ph/0102144] [INSPIRE].

[54] Particle Data Group collaboration, J. Beringer et al., *Review of particle physics (RPP)*, *Phys. Rev.* **D 86** (2012) 010001 [INSPIRE].

[55] E.H. Simmons, *Phenomenology of a technicolor model with heavy scalar doublet*, *Nucl. Phys.* **B 312** (1989) 253 [INSPIRE].

[56] S. Samuel, *Bosonic technicolor*, *Nucl. Phys.* **B 347** (1990) 625 [INSPIRE].

[57] A. Kagan and S. Samuel, *Renormalization group aspects of bosonic technicolor*, *Phys. Lett.* **B 270** (1991) 37 [INSPIRE].

JHEP01(2014)041

[58] C.D. Carone and E.H. Simmons, *Oblique corrections in technicolor with a scalar*, *Nucl. Phys.* **B 397** (1993) 591 [hep-ph/9207273] [INSPIRE].

[59] V. Hemmige and E.H. Simmons, *Current bounds on technicolor with scalars*, *Phys. Lett.* **B 518** (2001) 72 [hep-ph/0107117] [INSPIRE].

[60] M. Dine, W. Fischler and M. Srednicki, *Supersymmetric technicolor*, *Nucl. Phys.* **B 189** (1981) 575 [INSPIRE].

[61] M. Antola, S. Di Chiara, F. Sannino and K. Tuominen, *Minimal super technicolor*, *Eur. Phys. J.* **C 71** (2011) 1784 [arXiv:1001.2040] [INSPIRE].

[62] M. Antola, S. Di Chiara, F. Sannino and K. Tuominen, *Supersymmetric extension of technicolor & fermion mass generation*, *Nucl. Phys.* **B 864** (2012) 664 [arXiv:1111.1009] [INSPIRE].

[63] A. Manohar and H. Georgi, *Chiral quarks and the nonrelativistic quark model*, *Nucl. Phys.* **B 234** (1984) 189 [INSPIRE].

[64] A.G. Cohen, D.B. Kaplan and A.E. Nelson, *Counting 4π's in strongly coupled supersymmetry*, *Phys. Lett.* **B 412** (1997) 301 [hep-ph/9706275] [INSPIRE].

[65] R. Foadi and M.T. Frandsen, *Light Higgs from scalar see-saw in technicolor*, arXiv:1212.0015 [INSPIRE].

[66] R. Foadi, M.T. Frandsen and F. Sannino, 125 *GeV Higgs from a not so light technicolor scalar*, *Phys. Rev.* **D 87** (2013) 095001 [arXiv:1211.1083] [INSPIRE].

[67] CMS collaboration, *Combined results of searches for the Standard Model Higgs boson in pp collisions at $\sqrt{s} = 7$ TeV*, *Phys. Lett.* **B 710** (2012) 26 [arXiv:1202.1488] [INSPIRE].

[68] M. Bando, T. Kugo, S. Uehara, K. Yamawaki and T. Yanagida, *Is ρ meson a dynamical gauge boson of hidden local symmetry?*, *Phys. Rev. Lett.* **54** (1985) 1215 [INSPIRE].

[69] M. Bando, T. Kugo and K. Yamawaki, *Nonlinear realization and hidden local symmetries*, *Phys. Rept.* **164** (1988) 217 [INSPIRE].

[70] R. Foadi, M.T. Frandsen, T.A. Ryttov and F. Sannino, *Minimal walking technicolor: set up for collider physics*, *Phys. Rev.* **D 76** (2007) 055005 [arXiv:0706.1696] [INSPIRE].

[71] M.E. Peskin and T. Takeuchi, *A new constraint on a strongly interacting Higgs sector*, *Phys. Rev. Lett.* **65** (1990) 964 [INSPIRE].

[72] H.S. Fukano, M. Heikinheimo and K. Tuominen, *Flavor constraints in a bosonic technicolor model*, *Phys. Rev.* **D 84** (2011) 035017 [arXiv:1106.2433] [INSPIRE].

JHEP01(2014)041